Magnetic-field effects on quasi-two-dimensional excitons in coupled GaAs-(Ga,Al)As quantum wells

E. Reyes-Gómez,[1,2] L. E. Oliveira,[1] and M. de Dios-Leyva[2]

[1]*Instituto de Física, Unicamp, Caixa Postal 6165, Campinas, São Paulo, 13083-970, Brazil*
[2]*Department of Theoretical Physics, University of Havana, San Lázaro y L, Vedado 10400, Havana, Cuba*

We have used the variational procedure in the effective-mass and nondegenerate parabolic band approximations in order to investigate the effects of a magnetic field on the exciton effective mass and dispersion in semiconductor heterostructures. Calculations are performed for bulk GaAs, and two-dimensional and quasi-two-dimensional excitons in coupled GaAs-(Ga,Al)As quantum wells for applied magnetic fields perpendicular to the layers. A simple hydrogenlike envelope wave function provides the expected behavior for the exciton dispersion in a wide range of the center-of-mass momenta, and an analytical expression for the exciton effective mass is obtained. Present results lead to a magnetic-field dependent exciton effective mass and dispersion in quite good agreement with available experimental measurements in coupled GaAs-(Ga,Al)As quantum wells.

I. INTRODUCTION

In the last few decades a considerable amount of theoretical and experimental studies has been carried out on the exciton properties in multiple quantum well (QW) heterostructures. The central motivation of these studies has been the possible applications of these systems in optoelectronic devices. From the physical point of view, the main interest is concerned with the change of the physical properties of excitons when the electrons and holes are confined in different regions of the direct space or in different points of the inverse space. In particular, when the electron and hole are confined in the same space region and in the same point of the k space, the overlap of the single-particle wave functions is large as, for example, in a single QW heterostructure, and the exciton is called a direct exciton. On the other hand, it may happen that, due to the presence of confining potentials, the spatial separation of the electron and hole is such that it leads to a small overlap of the single-particle wave functions and to dramatic changes of the physical properties of the system, as in coupled double QW's: in this case, the exciton is referred to as an indirect exciton.

The application of a magnetic field on semiconductor heterostructures provides very useful band-structure data, and a variety of magneto-optical studies have been performed to obtain valuable experimental and theoretical information on exciton states under external magnetic fields. Most of the theoretical work in the literature do not take into account the coupling between the center-of-mass (c.m.) motion and the internal structure of the exciton. Gor'kov and Dzyaloshinskiĭ[1] have investigated the c.m./internal structure coupling for three-dimensional (3D) excitons and, more recently, a number of studies have been performed in order to investigate the influence of the exciton c.m. momentum on the exciton properties in the cases of two-dimensional (2D) and quasi-2D excitons.[2–14] For example, Paquet *et al.*[2] investigated the properties of a Bose condensate of noninteracting 2D magnetic excitons considering the influence of the mo-

tion of the particles in the direction perpendicular to the magnetic field, of the coupling to higher Landau levels, and of the spin-orbit interaction. By using magnetoabsorption and electroabsorption techniques, Fritze *et al.*[3] studied the effects of the applied magnetic fields parallel and perpendicular to the QW layers on the exciton behavior, and discussed how in-plane magnetic fields change the nature of the exciton by inducing a two-body velocity-dependent interaction. Bayer and co-workers[4] investigated the heavy-hole and light-hole excitons in coupled double QW's by photoluminescence (PL) and photoluminescence excitation (PLE) spectroscopy in magnetic fields up to 13 T. Other authors[5,6] studied the problem of the quasi-2D exciton in a transverse magnetic field, and obtained an expression for the exciton spectrum in an arbitrary field for a large separation between the confining-electron and -hole planes.[6] The effects of an in-plane magnetic field on the photoluminescence spectra in coupled QW's was also studied by Gorbatsevich and Tokatly[7] and Butov *et al.*,[8] and more recently by Chang *et al.*[11] Moreover, Parlangeli *et al.*[9] investigated the optical properties of GaAs/Al$_{0.35}$Ga$_{0.65}$As asymmetric double QW's under in-plane magnetic fields, and observed the energy-momentum dispersion of spatially indirect excitons.

Experiments of particular interest to this work were the studies by Butov *et al.*[10] and by Lozovik *et al.*,[13] who performed the first experimental measurements of the dispersion of a quasi-2D exciton in a coupled double GaAs/Al$_{0.33}$Ga$_{0.67}$As QW heterostructure under an external magnetic field, and indirectly obtained the exciton effective mass in the direction perpendicular to the magnetic field as a function of the applied field. They also formulated the quantum-mechanical problem of the quasi-2D exciton under an applied magnetic field and numerically solved[10,13,14] the Schrödinger equation in the imaginary-time formalism. The aim of the present work is to study 3D, 2D, and quasi-2D excitons, within a variational procedure which enables one to obtain a realistic exciton wave function in an analytical way, a clear advantage for performing calculations related to a

number of optical quantities associated with the exciton properties. Also, we shall obtain an analytical expression of the exciton effective mass in the direction perpendicular to the applied field by using the corresponding exciton variational wave function, and show that the present results lead to a magnetic-field-dependent exciton effective mass and dispersion in quite good agreement with available experimental measurements.[10,13]

The paper is organized as follows. In Sec. II we give our theoretical derivations for 3D, 2D, and quasi-2D excitons, propose the trial wave function to be used in the variational calculations, and obtain the analytical expression to evaluate the magnetic-field dependent exciton effective mass. Section III is concerned with the present theoretical results together with a discussion and comparison with experimental data[10,13] in coupled GaAs-$Ga_{0.67}Al_{0.33}$As QW's. Finally, our conclusions are given in Sec. IV.

II. THEORETICAL FRAMEWORK

We consider the problem of an exciton in a semiconductor heterostructure, grown along the z axis, under an applied magnetic field $\vec{B}$, within the effective-mass and nondegenerate-parabolic band approximations. If $\vec{A}(\vec{r})$ is the vector potential associated to the magnetic field, the Hamiltonian for the exciton may be given by

$$\hat{H} = \frac{1}{2m_e}\left(\hat{\vec{p}}_e + \frac{e}{c}\vec{A}_e\right)^2 + \frac{1}{2m_h}\left(\hat{\vec{p}}_h - \frac{e}{c}\vec{A}_h\right)^2$$
$$+ V_e(z_e) + V_h(z_h) - \frac{e^2}{\epsilon|\vec{r}_e - \vec{r}_h|}, \qquad (1)$$

where $\hat{\vec{p}}_e$, $\hat{\vec{p}}_h$ and m_e, m_h are the momentum operators and the effective masses of the electron and hole, respectively, V_e and V_h are the electron and hole confining potentials, respectively, e is the absolute value of the electron charge, ϵ is the dielectric constant (considered the same throughout the heterostructure), $\vec{A}_e = \vec{A}(\vec{r}_e)$ and $\vec{A}_h = \vec{A}(\vec{r}_h)$.

Introducing the operator associated to the exciton c.m. magnetic momentum[1]

$$\hat{\vec{P}} = \hat{\vec{p}}_e + \frac{e}{c}\vec{A}_e + \hat{\vec{p}}_h - \frac{e}{c}\vec{A}_h - \frac{e}{c}\vec{B} \times (\vec{r}_e - \vec{r}_h), \qquad (2)$$

it is easy to show that its three components commute between themselves, and it satisfies

$$\frac{d\hat{\vec{P}}}{dt} = -\nabla_e V_e(z_e) - \nabla_h V_h(z_h), \qquad (3)$$

which leads to the conservation of the $\hat{\vec{P}}_\perp = (\hat{P}_x, \hat{P}_y)$ transverse components of $\hat{\vec{P}}$. By assuming the magnetic field along the growth direction, and taking the symmetric gauge $\vec{A}(\vec{r}) = \frac{1}{2}\vec{B} \times \vec{r}$ for the vector potential, one may seek for simultaneous eigenfunctions of Eq. (1) and $\hat{\vec{P}}_\perp$ as[1]

$$\Psi(\vec{r}_e, \vec{r}_h) = \exp\left[\frac{i}{\hbar}\left(\vec{P}_\perp + \frac{e}{2c}\vec{B} \times \vec{r}\right) \cdot \vec{R}\right]\Phi_{\vec{P}_\perp}(\vec{\rho}, z_e, z_h), \qquad (4)$$

where $\vec{r} = \vec{r}_e - \vec{r}_h$ is the internal exciton coordinate, $\vec{\rho} = \vec{\rho}_e - \vec{\rho}_h$ is the in-plane internal exciton coordinate, $\vec{R} = (1/M)(m_e\vec{\rho}_e + m_h\vec{\rho}_h)$ is the in-plane exciton c.m. coordinate, $M = m_e + m_h$ is the total exciton mass, and $\Phi_{\vec{P}_\perp}$ satisfies

$$\left[\hat{H}_{ez} + \hat{H}_{hz} + \hat{H}_{2D} - \frac{e^2}{\epsilon r}\right]\Phi_{\vec{P}_\perp} = E_X\Phi_{\vec{P}_\perp}, \qquad (5)$$

where $r = \sqrt{\rho^2 + (z_e - z_h)^2}$ and

$$\hat{H}_{ez} = \frac{\hat{p}_{ez}^2}{2m_e} + V_e(z_e), \qquad (6a)$$

$$\hat{H}_{hz} = \frac{\hat{p}_{hz}^2}{2m_h} + V_h(z_h), \qquad (6b)$$

$$\hat{H}_{2D} = \frac{1}{2\mu}\hat{p}_\perp^2 + \gamma\frac{e}{2\mu c}\vec{B} \cdot (\vec{\rho} \times \hat{\vec{p}}_\perp)$$
$$+ \frac{e^2}{8\mu c^2}(\vec{B} \times \vec{\rho})^2 + \vec{F} \cdot \vec{\rho} + \frac{P_\perp^2}{2M}. \qquad (6c)$$

In the above equations, E_X is the exciton energy, μ is the exciton reduced mass, $\gamma = (m_h - m_e)/M$, $\hat{\vec{P}}_\perp = -i\hbar(\partial/\partial_{\vec{\rho}})$, and $\vec{F} = (e/Mc)\vec{P}_\perp \times \vec{B}$. Here we note that the dependence of the exciton energy on $\vec{P}_\perp$ is given by the last two terms in Eq. (6c), and that the term $\vec{F} \cdot \vec{\rho}$ represents the direct coupling between the c.m. and the in-plane internal exciton coordinate, i.e., it is determined by the interaction of the transverse electric dipole $-e\vec{\rho}$ with the electric field $(1/e)\vec{F}$ in the c.m. frame.

The conservation of $\vec{P}_\perp$ allow us to reduce the original problem with six degrees of freedom into one with only four degrees of freedom. Equation (5) will be used to study exciton properties in the 2D, quasi-2D, and 3D cases.

A. 3D exciton

For the 3D exciton, one may use Eq. (5) with $V_e = V_h = 0$. As a consequence, the z-component of the c.m. exciton momentum is also a constant of motion, and by introducing the c.m. coordinate $Z = (1/M)(m_e z_e + m_h z_h)$ and the relative coordinate $z = z_e - z_h$, one obtains

$$\hat{H}_{ez} + \hat{H}_{hz} = \frac{1}{2\mu}\hat{p}_z^2 + \frac{1}{2M}\hat{P}_z^2, \qquad (7)$$

where $\hat{p}_z = -i\hbar(\partial/\partial z)$ and $\hat{P}_z = -i\hbar(\partial/\partial Z)$. The last term of Eq. (7) only contributes by a constant to the exciton energy, and one may include it in E_X. The study of the 3D exciton then reduces to solving the problem

$$\hat{h}_{3D}\Phi_{\vec{P}_\perp}(\vec{r}) = E_X\Phi_{\vec{P}_\perp}(\vec{r}), \qquad (8)$$

with

$$\hat{h}_{3D} = \frac{1}{2\mu}\hat{p}_z^2 + \hat{H}_{2D} - \frac{e^2}{\epsilon r} \tag{9}$$

and $r = \sqrt{\rho^2 + z^2}$.

B. Quasi-2D and 2D excitons

As is well known, in a multiple QW heterostructure the electron and hole forming the exciton may be located in the same well or in different wells of the heterostructure, corresponding to direct or indirect excitons, respectively. If the wells of the heterostructure are deep and narrow, then the movement of the electron and hole may be considered as essentially 2D. Under these conditions, the properties of the exciton may be described by finding the solutions of the problem

$$\hat{h}_{2D}\Phi_{\vec{P}_\perp}(\vec{\rho}) = E_X \Phi_{\vec{P}_\perp}(\vec{\rho}) \tag{10}$$

with

$$\hat{h}_{2D} = \hat{H}_{2D} - \frac{e^2}{\epsilon r}, \tag{11}$$

where $r = \sqrt{\rho^2 + d^2}$, and d is the distance between the electron and hole confining planes. If $d=0$ the exciton is called a direct exciton or a 2D exciton, whereas if $d \neq 0$, the exciton is called an indirect exciton or a quasi-2D exciton.

C. Variational calculation

As one is not able to exactly solve Eqs. (8) and (10), approximated procedures are needed in order to obtain the exciton properties. In this sense, the variational procedure is a very useful tool for obtaining approximated solutions for the exciton problem under the influence of the heterostructure confining potential and applied external fields. We shall therefore use the variational scheme to obtain the ground state of 3D, 2D, and quasi-2D excitons under applied magnetic fields, and taking into account the effects of the c.m./internal structure coupling.

From Eq. (8) one may see that the exciton moves in an effective potential with two local minima separated by the vector[1,13]

$$\vec{\rho}_0 = \frac{c}{eB^2}\vec{B} \times \vec{P}_\perp, \tag{12}$$

one of that corresponding to the Coulomb potential and the other to the magnetic-parabolic potential. For a nonzero value of the applied magnetic field, and $\vec{P}_\perp = \vec{0}$, both minima coincide, and Eq. (8) may be approximately solved via the trial wave function[15]

$$\Phi_0(\vec{r}) = N_0 \exp\left[-\frac{\rho^2}{4l_B^2} - \lambda r\right], \tag{13}$$

where λ is a variational parameter, $l_B = \sqrt{\hbar c/eB}$ is the magnetic length, and N_0 is a normalization constant.

As $|\vec{P}_\perp| \to \infty$, $|\vec{\rho}_0| \to \infty$, and the properties of the exciton states are essentially determined by the magnetic-parabolic

potential.[1,13] In this case, the exciton wave function associated to the exciton ground state, with energy $\frac{1}{2}\hbar\omega_c$, is given by

$$\Phi_\infty(\vec{r}) = N_\infty \exp\left[i\frac{\gamma}{2\hbar}\vec{P}_\perp \cdot \vec{\rho} - \frac{(\vec{\rho} - \vec{\rho}_0)^2}{4l_B^2}\right], \tag{14}$$

where $\omega_c = eB/\mu c$ is the cyclotron frequency and N_∞ is a normalization constant. The above results suggests a trial wave function of the form

$$\Phi_{\vec{P}_\perp}(\vec{r}) = N \exp\left[i\frac{\gamma}{2\hbar}\vec{P}_\perp \cdot \vec{\rho} - \frac{(\vec{\rho} - \vec{\rho}_0)^2}{4l_B^2} - \lambda r\right] \tag{15}$$

to describe the exciton ground state associated to Eq. (8). We note that Eq. (15) leads to the correct behavior of E_X (Refs. 13 and 14) as $|\vec{P}_\perp| \to 0$ and $|\vec{P}_\perp| \to \infty$, and therefore one may expect that it would provide a good interpolation for the exciton energy as function of the in-plane c.m. momentum. The variational parameter λ is obtained via the minimization of

$$E_X(\lambda) = \langle\Phi_{\vec{P}_\perp}|\hat{h}_{3D}|\Phi_{\vec{P}_\perp}\rangle. \tag{16}$$

Of course, the wave function (15) may be used to describe the exciton ground state in the 2D and quasi-2D cases by taking $r = \sqrt{\rho^2 + d^2}$, together with a variational parameter obtained through the minimization of

$$E_X(\lambda) = \langle\Phi_{\vec{P}_\perp}|\hat{h}_{2D}|\Phi_{\vec{P}_\perp}\rangle. \tag{17}$$

Finally, in all cases the ground-state exciton energy E_X and the exciton binding energy E_B are related by

$$E_X = \frac{1}{2}\hbar\omega_c - E_B. \tag{18}$$

D. Exciton effective mass

Before obtaining the exciton effective mass, one may recall that both $\hat{h}_{2D}$ and $\hat{h}_{3D}$ remain invariant, for $\vec{P}_\perp = \vec{0}$, under the inversion of the spatial coordinates. As a consequence, the corresponding wave functions may be chosen with a defined parity and, therefore, the average of $\vec{\rho}$ is equal to zero in this case. On the other hand, for $\vec{P}_\perp \neq \vec{0}$, the operators $\hat{h}_{2D}$ and $\hat{h}_{3D}$ are invariants under simultaneous inversion of the spacial coordinates and $\vec{P}_\perp$, and therefore, $E_X(\vec{P}_\perp)$ is an even function of $\vec{P}_\perp$. Moreover, all terms in $\hat{h}_{2D}$ and $\hat{h}_{3D}$ are also invariant under an arbitrary rotation T around the z axis, with the exception of $\vec{F} \cdot \vec{\rho}$, which transforms according to the rule

$$\vec{F} \cdot T^{-1}\vec{\rho} = \frac{e}{Mc}(\vec{P}_\perp \times \vec{B}) \cdot T^{-1}\vec{\rho} = \frac{e}{Mc}(T\vec{P}_\perp \times \vec{B}) \cdot \vec{\rho}, \tag{19}$$

and therefore the dispersion $E_X(\vec{P}_\perp)$ depends approximately on $P_\perp^2$ for small values of $|\vec{P}_\perp|$, i.e., the c.m. momentum-dependence of the exciton energy is given by

$$E_X(\vec{P}_\perp) = E_X(\vec{0}) + \frac{P_\perp^2}{2M_X} \tag{20}$$

for small values of $|\vec{P}_\perp|$, where M_X is the exciton effective mass in the plane perpendicular to the applied magnetic field.

We shall obtain the M_X exciton effective mass by supposing that the exciton envelope wave function $\Phi_{\vec{P}_\perp}$ is exactly known. Then, according to the Hellmann-Feynman theorem[16]

$$\frac{\partial E_X(\vec{P}_\perp)}{\partial \vec{P}_\perp} = \left\langle \Phi_{\vec{P}_\perp} \left| \frac{\partial \hat{h}_\beta}{\partial \vec{P}_\perp} \right| \Phi_{\vec{P}_\perp} \right\rangle$$

$$= \frac{1}{M}\left(\vec{P}_\perp + \frac{e}{c}\vec{B} \times \langle \Phi_{\vec{P}_\perp} | \vec{\rho} | \Phi_{\vec{P}_\perp} \rangle \right), \tag{21}$$

with $\beta = 2D$, 3D and noticing that

$$\frac{\partial E_X(\vec{P}_\perp = \vec{0})}{\partial \vec{P}_\perp} = 0 \tag{22}$$

and

$$\frac{1}{M_X} = \frac{\partial^2 E_X(\vec{P}_\perp = \vec{0})}{\partial P_x^2} = \frac{\partial^2 E_X(\vec{P}_\perp = \vec{0})}{\partial P_y^2}, \tag{23}$$

it is straightforward to show that

$$\frac{1}{M_X} = \frac{1}{M}\left[1 - \frac{eB}{c}\frac{\partial}{\partial P_x}\langle \Phi_{\vec{P}_\perp} | y | \Phi_{\vec{P}_\perp} \rangle\right]_{\vec{P}_\perp = \vec{0}}$$

$$= \frac{1}{M}\left[1 + \frac{eB}{c}\frac{\partial}{\partial P_y}\langle \Phi_{\vec{P}_\perp} | x | \Phi_{\vec{P}_\perp} \rangle\right]_{\vec{P}_\perp = \vec{0}}. \tag{24}$$

Finally, by substituting Eq. (15) into Eq. (24), one obtains

$$M_X = \frac{M}{1 - \frac{\langle \rho^2 \rangle_0}{2l_B^2}}, \tag{25}$$

where $\langle \rho^2 \rangle_0 = \langle \Phi_{\vec{P}_\perp} | \rho^2 | \Phi_{\vec{P}_\perp} \rangle|_{\vec{P}_\perp = \vec{0}}$. Obviously, as $B \to 0$, $M_X \to M$ and one recovers the exciton total mass, as expected.

III. RESULTS AND DISCUSSION

We have calculated the ground-state exciton energy E_X [see Eq. (18)] as a function of the in-plane c.m. exciton momentum for different values of the applied magnetic field. The parameters we have used were $m_e = 0.067\, m_0$ and $m_h = 0.18\, m_0$ (m_0 is the free-electron mass) for the electron and heavy-hole effective masses, respectively,[17–19] and $\epsilon = 12.35$ for the GaAs dielectric constant. Theoretical results are shown in Fig. 1, with energies in units of the exciton Rydberg (R_y) and as a consequence, the exciton energy may be rewritten as $E_X/R_y = \gamma_B - E_B/R_y$, where $\gamma_B = \hbar\omega_c/2R_y$ is a quantity proportional to the magnetic field ($\gamma_B = 1$ corresponds to an applied magnetic field of ≈ 3.5 T). The in-plane c.m. momentum is $p = P_\perp/P_0$, in units of $P_0 = e^2 M/\epsilon\hbar$. One may distinguish two regimes for the exciton. The transition between these two regimes takes place at a certain value of
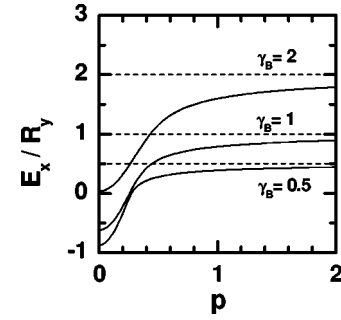
FIG. 1. 3D ground-state exciton energy (for bulk GaAs) in units of the exciton Rydberg as a function of the in-plane c.m. momentum for different values of the applied magnetic field. The magnetic fields are given in units of $\gamma_B = \hbar\omega_c/2R_y$ (notice dashed lines with the corresponding values of γ_B).

the c.m. momentum P_{tr} (or $p_{tr} = P_{tr}/P_0$), which is a function of the magnetic field as discussed by Lozovik *et al.*[13,14] When $p < p_{tr}$ the exciton behaves as an hydrogenlike system (hydrogenlike regime), whereas when $p > p_{tr}$ the exciton properties change abruptly (magnetoexciton regime). As $p \to \infty$ the exciton behaves as a free and uncorrelated electron-hole system whose energy is the sum of the lowest electron and hole Landau-level energies, i.e., $\frac{1}{2}\hbar\omega_c$ (or γ_B if the energy is expressed in R_y units; see Fig. 1). The behavior of the exciton properties as functions of the c.m. momentum may be understood in terms of the Lorentz' force acting separately upon the electron and hole. As p increases beyond of p_{tr} the electron-hole pair becomes more and more polarized, due to the increasing Lorentz' force. As a consequence, the Coulomb attraction between the electron and the hole falls more and more, and the exciton binding energy tends toward to zero. For small values of the c.m. momentum ($p < p_{tr}$), the effects of the Lorentz' force over the electron-hole pair are weak, and the exciton remains near to the condition of a hydrogenlike system.

Figure 2 shows the in-plane c.m. momentum dependence of the binding energy for the 3D [Fig. 2(a)], 2D [Fig. 2(b)], and quasi-2D excitons for $d = 0.5\, a_0$ and $d = a_0$ [Figs. 2(c) and 2(d) respectively], where a_0 is the exciton effective Bohr radius. Calculations were performed for different values of the applied magnetic field, starting with $B = 1$ T and increasing the field-value by 1 T until $B = 10$ T. As the exciton c.m. momentum increases the binding energy decreases, and tends towards zero as p tends to infinity. Of course, when the distance d (between the planes which confine the electron and hole) increases [Fig. 2(c) and 2(d)], the exciton binding energy decreases due to a smaller Coulomb interaction. However, when the magnetic field is increased, the exciton wave function becomes more localized for all values of the in-plane c.m. momentum, leading to an increase in the exciton binding energy. The magnetic-field dependence of the exciton binding energies is shown in Fig. 3. Figures 3(a) and 3(b) correspond to the 3D and 2D excitons, respectively, whereas Figs. 3(c) and 3(d) correspond to quasi-2D excitons with $d = 0.3\, a_0$ and $d = 0.5\, a_0$, respectively. Calculations were carried out for various values of the exciton c.m. momentum p. It is well known that the exciton binding energy depends on
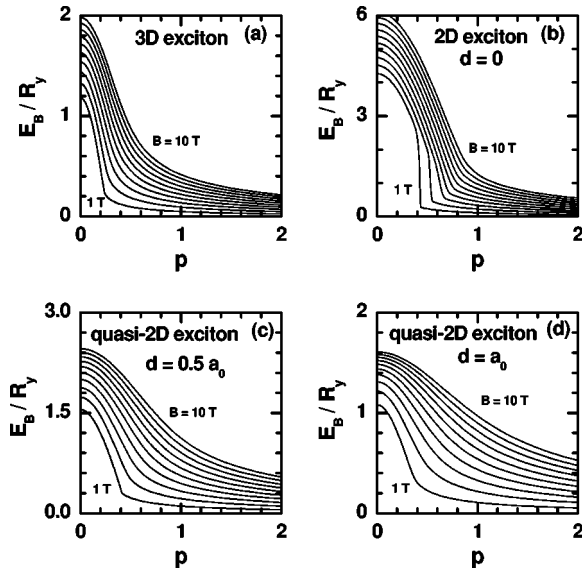
FIG. 2. Exciton binding energies as functions of the in-plane c.m. momentum for different values of the applied magnetic field (notice that full curves correspond to increasing values of 1 T from $B=1$ T to $B=10$ T). (a) corresponds to the 3D case, whereas (b) relates to the 2D case, and (c) and (d) to the quasi-2D exciton with $d=0.5$ a_0 and $d=a_0$, respectively, where a_0 is the exciton Bohr radius.

the magnetic field as $\sqrt{B}$ in the zero c.m. momentum limit.[10] When $p>p_{tr}$, this dependence changes abruptly, and for sufficiently large values of p the exciton binding energy transforms into a linear function of B with a decreasing slope when p is increased.

An important quantity related to the exciton wave function is the exciton probability density, which is closely re-
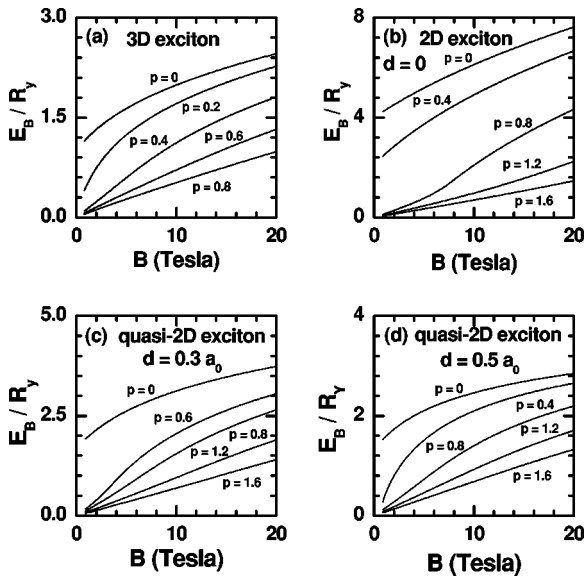
FIG. 3. Magnetic-field dependence of the exciton binding energies for different values of the in-plane c.m. momenta. (a) corresponds to the 3D case, whereas (b) relates to the 2D exciton, and (c) and (d) to the quasi-2D case with $d=0.3$ a_0 and $d=0.5$ a_0, respectively.
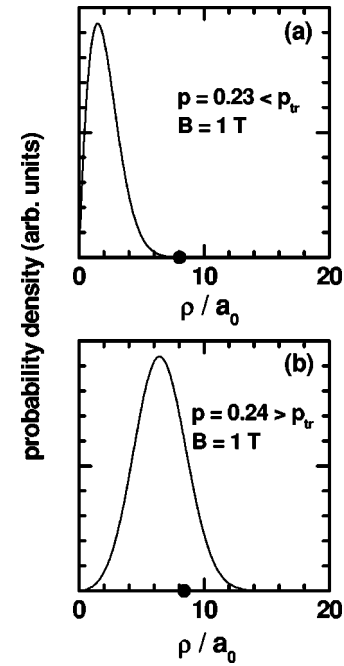
FIG. 4. Probability density $\rho|\Psi|^2$ for a 3D exciton as a function of the in-plane coordinate ρ. The probability density is evaluated at $\varphi=0$ and $z=0$. In (a) we show the hydrogenlike exciton regime, whereas in (b) we display the magnetoexciton regime. The full dot at the bottom axis is the position of the magnetic-orbit center.

lated to the localization properties of the exciton in real space. In Fig. 4 we examine the behavior of $\rho|\Psi_P|^2$, in cylindrical coordinates, as a function of ρ, for $z=0$ and $\varphi=0$, where $\rho=\sqrt{x^2+y^2}$ is the exciton in-plane coordinate, φ the axial angle, and z the coordinate in the magnetic-field direction. Results correspond to a 3D exciton for $B=1$ T, and for two different values of p at both sides of $p_{tr}\simeq0.235$. Full dots at the bottom axes represent the absolute value of $\vec{\rho}_0$, denoted as ρ_0, which is the distance from the origin of coordinates to the magnetic-orbit center. When $p<p_{tr}$ [see Fig. 4(a)] the probability density behaves as in the hydrogenlike case, as expected, whereas if $p>p_{tr}$ [see Fig. 4(b)] one may see a Gaussian profile of the probability density which is peaked near the magnetic-orbit center. These facts clearly illustrate the transition of the exciton from the hydrogenlike regime to the magnetoexciton regime.

As the in-plane c.m. momentum is increased, one may expect that the probability density peak position becomes closer to the magnetic-orbit center. As a consequence, one may also expect that the average of the exciton in-plane coordinate tends towards ρ_0 as p increases. Figure 5(a) shows the momentum dependence of the average $\langle\rho\rangle$ (solid lines) and of the magnetic-orbit center position ρ_0 (dashed lines) for different values of the magnetic field from $B=1$ T to $B=10$ T in steps of 1 T. Notice that in the limit $p\rightarrow\infty$ the average $\langle\rho\rangle$ tends towards ρ_0. In Fig. 5(b) it is shown the momentum dependence of the exciton quantum-confined Bohr radius,[20] defined as $a_X=\langle\Psi|1/r|\Psi\rangle^{-1}$, for the same values of the applied magnetic field used in Fig. 5(a). Notice that both $\langle\rho\rangle$ and a_X are measures of the exciton spatial extension. Again one may see the transition between the two
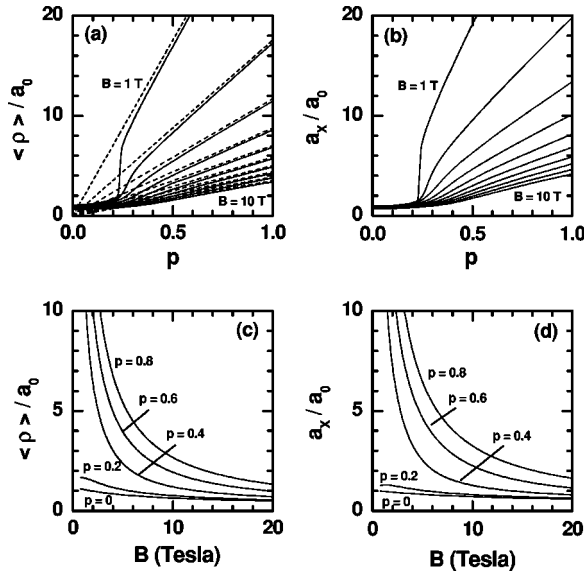
FIG. 5. Average of the in-plane coordinate $\rho=\sqrt{x^2+y^2}$ and of the quantum-confined Bohr radius for a 3D exciton as functions of the in-plane c.m. momentum for different values of the applied magnetic field [(a) and (b), respectively], and as functions of the applied magnetic field for various values of the c.m. momenta [(c) and (d), respectively]. Dashed lines in (a) correspond to the c.m. momentum dependence of ρ_0.

exciton regimes, and the linear-momentum dependence of $\langle\rho\rangle$ and a_X in the magnetoexciton regime. Obviously, the exciton becomes more spatially extended and polarized as p increases. Figures 5(c) and 5(d) show the average of $\langle\rho\rangle$ and of the exciton quantum-confined Bohr radius as functions of the applied magnetic field, respectively, for different values of p. In the hydrogenlike regime the magnetic-field dependence of $\langle\rho\rangle$ and a_X is quite slow, whereas in the magnetoexciton regime these magnitudes depend hyperbolically on the magnetic field. Results from Fig. 5 were performed for a 3D GaAs exciton, and we note that results obtained for 2D and quasi-2D excitons, although not shown here, are very similar.

We have also compared our theoretical calculations with some of the experimental data previously reported. In Fig. 6, full dots correspond to the experimental results from Butov et al.[10] and Lozovik et al.,[13] who studied the dispersion of an indirect exciton in GaAs/Ga$_{0.67}$Al$_{0.33}$As double-coupled QW's. Moreover, they have determined a mean interlayer separation in the indirect exciton regime corresponding to $d=115$ Å which is close to the distance between the QW centers. The experimental data are therefore compared with the present theoretical calculations (solid lines) for a quasi-2D exciton with $d=115$ Å and for the magnetic-field values in the experiment. We included in the exciton-peak energy the effects of the heterostructure confining potential by summing the electron and hole confining energies to the exciton energy and gap energy, according to the sample specifications done by Butov et al.[10] Notice the good agreement between experimental measurements and present calculations. For a better quantitative agreement between experimental and theoretical results, one may explicitly include in the exciton Hamiltonian the electron and hole confining po-
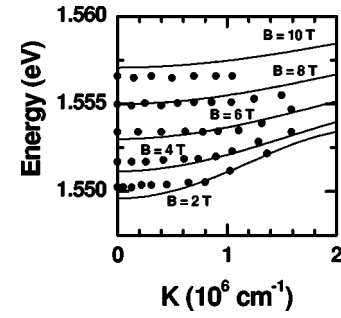
FIG. 6. Exciton dispersion for different values of the applied magnetic field. Here $K=P_\perp/\hbar$ is in units of 10^6 cm^{-1}. Solid lines represent present calculations for the quasi-2D case with $d=115$ Å, whereas full dots correspond to the experimental results from Butov et al. (Ref. 10) and Lozovik et al. (Ref. 13) in coupled GaAs-Ga$_{0.67}$Al$_{0.33}$As QW's.

tentials, and propose a more realistic variational wave function for the exciton ground state.

Finally, we display in Fig. 7 the magnetic-field dependence of the exciton effective mass, expressed in units of the free-electron mass [$m=M_X/m_0$, see Eq. (25)], for 2D (dashed line), 3D (doted line), and quasi-2D (solid line) excitons. Full dots correspond to the experimental results from Butov et al.[10] and Lozovik et al.[13] for an indirect exciton in a GaAs/Ga$_{0.67}$Al$_{0.33}$As double-coupled QW with $d=115$ Å. Our theoretical calculation corresponding to the quasi-2D exciton was also performed for $d=115$ Å, according to the experimental specifications. Notice that, in all cases, the exciton effective mass increases when the magnetic field is increased. In the case of a quasi-2D exciton, for large values of the magnetic field the discrepancy between the theoretical curve and the experimental points becomes larger. This problem may be solved, in part, by including in the theoretical model the effects of the double-coupled QW confining potential.

IV. CONCLUSIONS

In summary, we have solved the Schrödinger equation corresponding to the 3D, 2D, and quasi-2D excitons by using
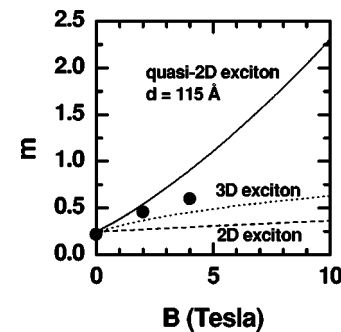
FIG. 7. Exciton effective mass $m=M_X/m_0$ as a function of the magnetic field for 2D (dashed line), 3D (dot line), and quasi-2D (solid line) excitons. Full dots correspond to the experimental results from Butov et al. (Ref. 10) and Lozovik et al. (Ref. 13) in coupled GaAs—Ga$_{0.67}$Al$_{0.33}$As QW's.

the variational procedure. We proposed a simple hydrogen-like trial wave function, which provides the correct behavior[13,14] of the calculated magnitudes in the limit $p \rightarrow 0$ and $p \rightarrow \infty$, and that is very useful in order to carry out calculations, for example, of the optical magnitudes related to the exciton properties. We also obtained an analytical expression to evaluate the exciton effective mass by using the proposed variational wave function. Present theoretical results for the exciton dispersion and for exciton effective mass were found in good agreement with experimental data in coupled $GaAs$-$Ga_{0.67}Al_{0.33}As$ QW's. Of course, a better correspondence between experimental and theoretical results would be obtained if one includes both the effects of the confining potential as well as of the complex band structure in the theoretical calculations.

[1] L. P. Gor'kov and I. E. Dzyaloshinskiǐ, Sov. Phys. JETP **26**, 449 (1968).

[2] D. Paquet, T. M. Rice, and K. Ueda, Phys. Rev. B **32**, 5208 (1985).

[3] M. Fritze, I. E. Perakis, A. Getter, W. Knox, K. W. Goosen, J. E. Cunningham, and S. A. Jackson, Phys. Rev. Lett. **76**, 106 (1996).

[4] M. Bayer, V. B. Timofeev, F. Faller, T. Gutbrod, and A. Forchel, Phys. Rev. B **54**, 8799 (1996).

[5] A. Imamoḡlu, Phys. Rev. B **54**, R14 285 (1996).

[6] Yu. E. Lozovik and A. M. Ruvinskiǐ, JETP **85**, 979 (1997).

[7] A. A. Gorbatsevich and I. V. Tokatly, Semicond. Sci. Technol. **13**, 288 (1998).

[8] L. V. Butov, A. V. Mintsev, Yu. E. Lozovik, K. L. Campman, and A. C. Gozzard, Phys. Rev. B **62**, 1548 (2000).

[9] A. Parlangeli, P. C. M. Christianen, J. C. Maan, C. B. Soerensen, and P. E. Lindelof, Phys. Status Solidi A **178**, 45 (2000); A. Parlangeli, P. C. M. Christianen, J. C. Maan, I. V. Tokatly, C. B. Soerensen, and P. E. Lindelof, Phys. Rev. B **62**, 15 323 (2000).

[10] L. V. Butov, C. W. Lai, D. S. Chemla, Yu. E. Lozovik, K. L. Campman, and A. C. Gossard, Phys. Rev. Lett. **87**, 216804 (2001).

[11] Kai Chang and F. M. Peeters, Phys. Rev. B **63**, 153307 (2001); Kai Chang, J. B. Xia, H. B. Wu, and S. L. Feng, Appl. Phys. Lett. **80**, 1788 (2002).

[12] N. E. Kaputkina and Yu. E. Lozovik, Physica E (Amsterdam) **12**, 323 (2002).

[13] Yu. E. Lozovik, I. V. Ovchinnikov, S. Yu. Volkov, L. V. Butov, and D. S. Chemla, Phys. Rev. B **65**, 235304 (2002).

[14] Yu. E. Lozovik and S. Yu. Volkov, JETP **96**, 564 (2003).

[15] E. Reyes-Gómez, L. E. Oliveira, and M. de Dios-Leyva, Semicond. Sci. Technol. **19**, 699 (2004).

[16] C. Cohen-Tannoudji, B. Diu, and F. Laloe, *Quantum Mechanics* (Wiley, Paris, 1977), Vol. II.

[17] L. C. Andreani, A. Pasquarello, and F. Bassani, Phys. Rev. B **36**, 5887 (1987).

[18] G. E. W. Bauer and T. Ando, Phys. Rev. B **38**, 6015 (1998).

[19] R. P. Leavitt and J. W. Little, Phys. Rev. B **42**, 11 774 (1990).

[20] F. Rossi, G. Goldoni, and E. Molinari, Phys. Rev. Lett. **78**, 3527 (1997); Y. Zhang and A. Mascarenhas, Phys. Rev. B **59**, 2040 (1999).